

Published in final edited form as:

*Methods Enzymol.* 2014 ; 537: 123–139. doi:10.1016/B978-0-12-411619-1.00007-0.

## Use of Osmium Tetroxide Staining with Microcomputerized Tomography to Visualize and Quantify Bone Marrow Adipose Tissue *In Vivo*

Erica L. Scheller<sup>\*,1</sup>, Nancy Troiano<sup>†,1</sup>, Joshua N. VanHoutan<sup>‡,1</sup>, Mary A. Bouxsein<sup>§</sup>, Jackie A. Fretz<sup>†</sup>, Yougen Xi<sup>†</sup>, Tracy Nelson<sup>†</sup>, Griffin Katz<sup>†</sup>, Ryan Berry<sup>¶</sup>, Christopher D. Church<sup>¶</sup>, Casey R. Doucette<sup>||</sup>, Matthew S. Rodeheffer<sup>¶</sup>, Ormond A. MacDougald<sup>\*</sup>, Clifford J. Rosen<sup>||</sup>, and Mark C. Horowitz<sup>†,2</sup>

<sup>\*</sup>Department of Molecular and Integrative Physiology, University of Michigan, Ann Arbor, Michigan, USA

<sup>†</sup>Department of Orthopaedics and Rehabilitation, Yale University School of Medicine, New Haven, Connecticut, USA

<sup>‡</sup>Department of Internal Medicine, Endocrinology, Yale University School of Medicine, New Haven, Connecticut, USA

<sup>§</sup>Center for Advanced Orthopedic Studies, Beth Israel Deaconess Medical Center and Harvard Medical School, Boston, Massachusetts, USA

<sup>¶</sup>Section of Comparative Medicine, Yale University School of Medicine, New Haven, Connecticut, USA

<sup>||</sup>Maine Medical Center Research Institute, Scarborough, Maine, USA

### Abstract

Adipocytes reside in discrete, well-defined depots throughout the body. In addition to mature adipocytes, white adipose tissue depots are composed of many cell types, including macrophages, endothelial cells, fibroblasts, and stromal cells, which together are referred to as the stromal vascular fraction (SVF). The SVF also contains adipocyte progenitors that give rise to mature adipocytes in those depots. Marrow adipose tissue (MAT) or marrow fat has long been known to be present in bone marrow (BM) but its origin, development, and function remain largely unknown. Clinically, increased MAT is associated with age, metabolic diseases, drug treatment, and marrow recovery in children receiving radiation and chemotherapy. In contrast to the other depots, MAT is unevenly distributed in the BM of long bones. Conventional quantitation relies on sectioning of the bone to overcome issues with distribution but is time-consuming, resource intensive, inconsistent between laboratories and may be unreliable as it may miss changes in MAT volume. Thus, the inability to quantitate MAT in a rapid, systematic, and reproducible manner has hampered a full understanding of its development and function. In this chapter, we describe a new technique that couples histochemical staining of lipid using osmium tetroxide with

microcomputerized tomography to visualize and quantitate MAT within the medullary canal in three dimensions. Imaging of osmium staining provides a high-resolution map of existing and developing MAT in the BM. Because this method is simple, reproducible, and quantitative, we expect it will become a useful tool for the precise characterization of MAT.

## 1. INTRODUCTION

“If the marrow were a nicely isolated organ like the spleen its study would certainly become much less time consuming” (Oehlbeck, Robscheit-Robbins, & Whipple, 1932). This quote from 1932 emphasizes a problem that has been faced by bone biologists for decades; analysis of the bone marrow (BM) requires one to first deal with the bone. This explains why most of the work in the late 1800s and early 1900s was anatomical in nature and relied on large specimens from human cadavers. Bone of this size could be sectioned for visual comparison without major disruption of the marrow elements. Optimization of decalcification protocols for downstream histological analysis from the late 1920s to early 1940s expanded our appreciation of the cellular content and morphology of the BM, including its tendency to contain a large number of adipocytes (Kramer & Shipley, 1927; Lillie, 1944). Distribution of the marrow adipose tissue (MAT) in the skeleton is a tightly regulated process while its origin and function remain largely unknown.

Quantitation of MAT in mice has historically been accomplished by counting adipocyte “ghosts” in serial histological sections of paraffin or plastic embedded bone. This method is time-consuming, resource intensive, and subject to significant variation because of interlaboratory variation and because MAT is not evenly distributed throughout the medullary canal (Fig. 7.1). If adequate analysis is not performed, traditional sectioning methods can easily miss changes in MAT volume and/or distribution. In species ranging in size from rat to humans indirect imaging techniques, including computed tomography and magnetic resonance (MR) spectroscopy, have been applied with success (Bredella et al., 2009; Demontiero, Li, Thembani, & Duque, 2011; Regis-Arnaud et al., 2011). Although MR has been tried in isolated mouse femurs, quantitation of fat versus water is very imprecise (C.J. Rosen, unpublished). Thus, the inability to quantitate MAT in a rapid, systematic, and reproducible manner in a variety of mouse models has hampered a full understanding of MAT development, distribution, and function. To overcome this limitation, in this chapter we present a simple method that couples histochemical staining of lipid using osmium tetroxide with microcomputerized tomography (micro-CT) for rapid three-dimensional quantification of MAT.

### 1.1. Accumulation and distribution of MAT

Since 1882 it has been well documented that in early childhood the BM exists in a predominantly red or hematopoietic state (Custer, 1932). In addition, it is now known that this same BM, in addition to being hematopoietic, is also osteogenic. MAT infiltration accelerates shortly after birth in the distal portions of the appendicular skeleton before developing in more proximal areas (Emery & Follett, 1964). For example, in humans the BM of the middle phalanges of the toes is completely converted to MAT by 12 months of age (Emery & Follett, 1964). This process results in filling of peripheral bones with

“yellow” fatty marrow (i.e., hands, feet, tibia) while central bones retain red hematopoietic/osteogenic marrow throughout life (i.e., pelvis, ribs, lumbar vertebrae). By age 25 human BM is approximately 70% MAT, at which point its rate of accumulation slows markedly but continues throughout life (Custer & Ahlfeldt, 1932). In human adults, males generally have more MAT than females (Shillingford, 1950). This is also true in inbred strains of mice. However, the amount of MAT particularly in the long bones is strain-dependent (M.C. Horowitz, C.J. Rosen, & C.R. Farber, unpublished). Consistent with human findings, in 1889 Ranvier recorded the presence of a MAT gradient in the vertebrae of rats ranging from predominantly cellular, red marrow in the lumbar vertebrae to fatty, yellow marrow in the tail (Huggins & Blocksom, 1936; Ranvier, 1889). This historical finding has since been reobserved in mice and used as the basis for studies of MAT regulation of bone formation and hematopoiesis (Naveiras et al., 2009; Wronski, Smith, & Jee, 1981).

MAT may exist in at least two forms. The first population, “constitutive” MAT (cMAT), corresponds with areas of early MAT formation such as the distal tibia, feet, or caudal vertebrae. The second type, “regulated” MAT (rMAT), tends to develop with aging and is located interspersed with hematopoietic cells at sites such as the distal femur and proximal tibia in mice or the proximal femur and lumbar vertebrae in humans. The underpinning of this observation was published in 1976 when it was determined histologically that populations of cMAT fail to stain with performic acid–Schiff (PFAS) while their regulated counterparts readily display the characteristic red staining pattern (Tavassoli, 1976b). This implies that not only is the lipid composition different, the two populations also have differential abilities to respond to regulatory cues linked to induction of hematopoiesis. Like osmium staining, the PFAS reaction relies on the oxidation of carbon–carbon double bonds in unsaturated lipids indicating that rMAT, at least in rabbits, contains a higher proportion of unsaturated fatty acids (FAs) than cMAT. As both populations of adipocytes contain unsaturated FAs, it is likely that longer staining times with PFAS (as with osmium) would result in staining of the majority of the marrow adipocytes. It is possible that with time rMAT can mature into cMAT. This may explain observations that MAT maturation with age is associated with a decrease in the level of unsaturated FAs and implies that it is more difficult to shed MAT in favor of hematopoiesis as we age (Yeung et al., 2005).

## 1.2. Metabolic function of MAT

During the early 1900s, the rabbit emerged as the main animal model for the study of MAT due to its high proportion of fatty marrow and ease of MAT access and manipulation. The existence of saturated FAs within BM was documented in the early 1930s, followed by polyunsaturated FAs in the 1940s, and a more detailed breakdown that corresponds with recent results was published in 1954 (Evans, Riemenschneider, & Herb, 1954). During the 1960s, an interest in comparing the metabolic function of the marrow adipocyte to the peripheral white adipocyte began to emerge. This is reflected by publications such as the dissertation of Shore in 1969 entitled “Bone Marrow as an Adipose Tissue” reaffirming the thought that MAT may represent a metabolically relevant depot (Shore, 1969). Subsequent work in the 1970s revealed that the marrow fat cell in rabbits is four to six times smaller in volume than that of the perinephric white adipose tissue (WAT) adipocyte (Bathija, Davis, & Trubowitz, 1979; Trubowitz & Bathija, 1977). This is in accordance with our

measurements comparing adipocyte size in MAT and gonadal WAT in mice; however, when compared to subcutaneous WAT, the MAT adipocyte was larger in size (O.A. MacDougald, unpublished).

Metabolic function was examined by measuring rates of  $^{14}\text{C}$ -palmitate turnover in rabbit MAT and perinephric WAT (Trubowitz & Bathija, 1977). Injection of labeled palmitate, a free FA, into the circulation allows analysis of its rate of incorporation into triglyceride and is a measure of triglyceride synthesis by the adipose tissue. Incorporation of  $^{14}\text{C}$ -palmitate was five times greater in MAT than in perinephric WAT likely reflecting an increase in the number of adipocytes per tissue volume (Trubowitz & Bathija, 1977). Strikingly, fasting of rabbits for up to 3 weeks did not diminish the FA esterification capacity of the MAT, while that of the perinephric WAT decreased by as much as 60% (Bathija et al., 1979). In his seminal work with fasted rabbits, Tavassoli found that after 10 days of food restriction electron microscopic analysis revealed marked breakdown of the central lipid vacuole in WAT adipocytes while MAT cells of the distal tibia failed to undergo fat mobilization (Tavassoli, 1974). We have observed the same phenomenon at the light microscopic level in mice fasted for 24 h when comparing MAT from caudal vertebrae to gonadal WAT and subcutaneous WAT (O.A. MacDougald, unpublished). Of note, both of these regions (distal tibia and caudal vertebrae) are cMAT depots. This observation has been supported in recent years by the finding that unlike peripheral WAT, MAT has the capacity to increase in states of calorie restriction and conditions such as anorexia nervosa (Bredella et al., 2009; Devlin et al., 2010; Fazeli et al., 2013). These findings suggest that while MAT readily esterifies and stores FA as triglyceride, similar to metabolically active WAT, it does not respond in the same way to nutritional status.

### 1.3. Origin of the marrow adipocyte

Elegant ultrastructural studies of developing adipocytes in BM and peripheral WAT in 1976 demonstrated that the cellular origin of BM adipose tissue differs from that of extramedullary WAT (Tavassoli, 1976a). While the WAT progenitors were characterized as “fibroblast-like” with abundant rough endoplasmic reticulum and a close association with large amounts of collagen, the MAT progenitor only occasionally contained profiles of rough ER and was not associated with collagen (Tavassoli, 1976a). Recently, WAT progenitors have been identified *in vitro* and *in vivo* as a WAT-resident stromal cell population with the cell surface phenotype  $\text{Pdgfra}^+ \text{Lin}^- \text{CD29}^+ \text{CD34}^+ \text{Sca1}^+ \text{CD24}^+$  (Berry & Rodeheffer, 2013; Rodeheffer, Birsoy, & Friedman, 2008). Consistent with the hypothesis from 1976, this WAT-specific progenitor population is not present within mouse BM (M.C. Horowitz & M.S. Rodeheffer, unpublished). This reinforces the notion that MAT arises from a unique progenitor population that has yet to be fully identified. However, using lineage tracing, the BM adipocyte progenitor also expresses  $\text{Pdgfra}$  (M.C. Horowitz & M.S. Rodeheffer, unpublished).

### 1.4. Summary

Osmium tetroxide was first introduced by Palade (1952) for his classic work identifying the structure and function of cell organelles using the electron microscope. Osmium tetroxide (osmic acid) is one of the oldest fat stains and unsaturated FAs like oleic acid have been

traditionally considered to be responsible for the reduction reaction. Osmium tetroxide is soluble in fats and forms a black reduction compound with them by the addition to the double carbon-to-carbon bonds. In a manner similar to Palade, we reasoned that because osmium is a heavy metal and therefore radiodense, it will appear opaque to CT and as a result can be visualized.

In recent decades, accumulation of MAT has been strongly associated with metabolic disease and development of osteoporosis (Fazeli et al., 2013). However, the time-consuming nature of MAT quantification and analysis in mice has limited our understanding of its origin and physiology. The osmium staining technique for quantification of MAT in three dimensions is an exciting new tool that will help to increase our understanding of the distribution and development of MAT and allow us to further characterize its relationship to bone formation, hematopoiesis, and systemic metabolism.

## 2. MATERIALS

### 2.1. Mice

Strains C57BL/6 (B6), C3H/HeJ (C3H) BALB/c, AZIP lipodystrophic mice (Moitra et al., 1998), FVB (background strain for AZIP), and *Ebfl*<sup>-/-</sup> (B6 × 129 background) (Fretz et al., 2010) have been analyzed. Mice from 4 to 52-weeks old have been used successfully.

*Note:* Although we have not tested all mouse strains, strain B6 has the lowest bone density while C3H has the highest bone density of all mouse strains. Efficient staining is dependent on penetration of the osmium into the medullary canal. The penetration is partially dependent on the amount of decalcification. Because we have successfully stained C3H, we believe any mouse strain can be assessed using this method.

Due to the poor penetration of osmium, staining of marrow adipocytes in larger bones (i.e., rat and rabbit) has several limitations. If a decalcified rat bone is stained with osmium, even for several days, only the outermost perimeter of marrow adipocytes is stained. This phenomenon is also observed when attempting to stain rabbit bones. For rats, this can be overcome by taking a 0.8–1 mm horizontal slice of bone and marrow after decalcification in your area of interest. If this slice is stained in 1% osmium tetroxide under vacuum for 24 h, the osmium stain will penetrate approximately 0.5 mm from each direction and is then suitable for CT analysis. This allows for three-dimensional marrow fat quantification in a defined region of larger bones.

### 2.2. Dissecting tools

Operating scissors 51/2' straight #70-2070, Biomedical Research Instruments, Rockville, MD

Operating scissors 41/2' straight #70-2010, Biomedical Research Instruments, Rockville, MD

### 2.3. Glassware and plastic ware

Shandon Cassette I Biopsy, #1000969, Thermo Fisher Scientific, Kalamazoo, MI; 20 ml disposable glass scintillation vials.

### 2.4. Preparation of decalcification solution

Prepare in advance

- 41.4 g EDTA (ethylenediamine tetraacetic acid, disodium salt dehydrate, Fisher #S311-500)+4.4 g NaOH
- QS to 1000 ml dH<sub>2</sub>O (gentle heating to dissolve EDTA); adjust pH to 7.0–7.4

### 2.5. Preparation of osmium tetroxide staining solution

*IMPORTANT* osmium is very dangerous. *ALL WORK* with osmium *MUST* be done in a properly functioning fume hood. *DO NOT* get osmium on your skin—wear gloves. *VAPORS are DANGEROUS* and will damage your mucous membranes and your corneas (lachrymator).

Osmium tetroxide 2% aqueous solution from Polysciences Inc, Warrington, PA (#23311). The osmium tetroxide comes in 5 ml sealed glass vials. The vials *MUST* be opened in a fume hood.

- 5% potassium dichromate (5 g of potassium dichromate in 100 ml distilled water)
- Prepare fresh each time you stain:
- Mixed in glass scintillation vials.
- 1 part 5% potassium dichromate (stabilizing agent; included to prevent the reduction of the osmium).
- 1 part 2% osmium tetroxide
- Final concentration 1%

## 3. METHODS

### 3.1. Isolation of mouse long bones

**3.1.1 Mouse dissection**—Male or female mice of any age can be used. We have examined mice as young as weaning age (21–28 days) to as old as 6 months. We routinely use mice 6–16 weeks old.

1. Euthanize mice by CO<sub>2</sub> asphyxiation and cervical dislocation; or by other methods acceptable to your animal use committee.
2. Wet the hair of the euthanized mouse with 70% ethanol to flatten the hair. Using scissors (operating scissors 5 1/2' straight #70-2070, Biomedical Research Instruments, Rockville, MD) make a single cut through the hair and skin just behind the head, on the neck and strip-off the skin the length of the body, pulling the skin over the hind legs and feet.

3. Using scissors, and as a guide, the flexion of the leg at its attachment to the body, cut deep into the pelvic joint (femur–pelvis), keeping the femoral head intact, freeing the leg from the rest of the body. Cut off the foot just below the ankle and place in a 100 mm sterile tissue culture or Petri dish.
4. Remove as much soft tissue (tendons, ligaments, and muscle) as possible using scissors (operating scissors 41/2' straight #70-2010, Biomedical Research Instruments, Rockville, MD). This is important, because the less soft tissue that remains attached to the bone, the less superfluous tissue that will be stained and thus visualized by osmium. It is important, at this point, to keep the knee joint intact.

*Note:* It has been our experience that using a Kimwipe or gauze to manipulate the soft tissue, especially the muscle, facilitates the removal of the tissue. Not all the tissue can be removed.

5. Using a scalpel with a number 15 blade, separate the tibia from the femur.

*Note:* It has been our experience that inserting the blade into the knee joint and manipulating the blade side to side with light pressure ensures the joint separates without cutting off the epiphysis and damaging the growth plate.

*Note:* Bones are NEVER to be frozen.

### 3.2. Fixation of the bone

1. Place bones in tissue processing cassettes (Shandon Cassette I Biopsy, #1000969, Thermo Fisher Scientific, Kalamazoo, MI). Place the cassettes in a large plastic or glass beaker, and immediately immerse the bones in 10% neutral buffered formalin (Fisher #SF100-4). The volume of formalin should be sufficient to more than cover the cassettes. For small numbers of bones, a tibia and femur can be fixed in a small tube in 2.0 ml of formalin (volume of formalin 103 the bone volume (BV)). Fix the bones overnight at 4 °C with gentle agitation.

*Note:* It is important to exclude organic compounds (e.g., ethanol) in the fixative due to their lipid soluble capacity.

2. The next day, pour off the formalin, rinse 1× with cool tap water, and then wash the fixed bones for 1 h in running cool tap water.

*Note:* Although we have not done a side-by-side comparison, it is our experience that washing out the formalin the next day gives excellent results compared to leaving the bones in formalin for long periods of time. We recommend not leaving the bones in formalin for more than 3 days; longer periods of time result in more brittle bones.

### 3.3. Decalcification of the bones

1. Remove the cassettes from the wash, shake off the excess water, and immerse in the EDTA decalcification solution (decal). The volume of EDTA should be sufficient to more than cover the cassettes.

2. Decal is done at 4 °C with gentle agitation. After the first 24 h, pour off the decal and exchange with fresh decal.
3. The decal is then changed every 3–4 days until the bones are ready (~14 days) for staining.

*Note:* 14 days in decal is appropriate for most mouse bones (tibia and femur). Decal is done to remove mineral to allow optimal penetration of the osmium. Because different mouse strains have different bone densities (amounts of mineral/BV), it may be necessary to adjust the time in decal. It has been our experience that 10 days is a minimum and we have not had the bones in decal past 17 days. By 17 days, the bones are flexible to the touch.

4. Pour off the decal, rinse the cassettes 1× in cool tap water and then wash the cassettes for 1 h in cool running tap water.

### 3.4. Osmium staining of the decalcified bones

*IMPORTANT*, osmium tetroxide is very dangerous. *ALL WORK* with osmium *MUST* be done in a fume hood. *DO NOT* get osmium tetroxide on your skin—wear gloves. Wear a laboratory coat and no open toed shoes. *VAPORS are DANGEROUS* and will damage your mucous membranes and your corneas (lachrymator).

1. Remove the decalcified bones from the cassettes using forceps. For the tibia, cut off the bone just proximal to the ankle joint and place the bone in plastic screw-cap CryoTube vials (Thermo Scientific #363401, Denmark) with the cut-end up (proximal tibia facing down in the tube). Glass vials can also be used. For the femur, cut off the bone just below the femoral head and place in the vial with the cut-end up (distal femur facing down in the tube). A maximum of four bones can be placed in a single tube.

*Note:* Placing the bone with the cut end facing up is done to allow maximal penetration of the osmium. If analysis of the distal tibia or proximal femur is required, the end of the bones can be left intact. However, staining time may have to be increased.

2. Incubate the bones with the osmium tetroxide for 48 h at room temperature **IN THE FUME HOOD**.
3. Use forceps to retrieve the bones from the staining vials and place bones in new cassettes and wash under cool running tap water for 2 h.
4. Dispose of osmium liquid waste and glass or plastics contaminated with osmium as recommended by your institution.

*Note:* A careful histological examination of the osmium-stained sections reveals staining only in the adipocytes. No staining could be seen in the smaller hematopoietic cells. This suggests the vast majority of the osmium staining is focused in the adipocytes.



### 3.5. Microcomputed tomography

Micro-CT was performed in water with energy of 55 kVp, an integration time of 500 ms, and a maximum isometric voxel size of 10  $\mu\text{m}$  (the “high”-resolution setting with a 20 mm sample holder) using a micro-CT-35 (Scanco Medical, Bruttisellen, Switzerland). We increase throughput by using a 20 mm diameter sample holder and placing bones evenly in rows, separated by moist cotton, in seven standard drinking straws arrayed six around the perimeter and one in the center of the tube. Using this setup, at least 28 bones can be scanned at one time in batch mode. When creating volumes of interest (VOI), the interface between the decalcified bone and the MAT is usually apparent, facilitating placement of graphical objects. When segmentation is applied, MAT can be visualized unencumbered by the surrounding bone (Fig. 7.2A). To determine the position of the MAT within the medullary canal and to determine its change in volume, the bone can be overlaid (Fig. 7.2B). using this method, striking differences in MAT can be seen over the length of the femur between B6 (Fig. 7.3A) and C3H (Fig. 7.3B) mice. The MAT is so prevalent in C3H that it fills the fibula (thin line to the right of the tibia). In our hands, B6 mice have the lowest MAT while C3H have the highest of any of the strains we have tested.

Scanning the entire length of the bone is time consuming, although may be necessary depending on the experimental requirements. To reduce scanning time, we have selected four VOI: (1) above the growth plate in the secondary center of ossification, (2) just below the growth plate, (3) down the shaft in the metaphysis, and (4) in the diaphysis. Four VOI within the marrow space, extending 230  $\mu\text{m}$ , were defined by their position along the  $z$ -axis (Fig. 7.4). The first VOI began 460  $\mu\text{m}$  from the proximal end of the tibia, and each subsequent VOI began 1.2 mm distal to the previous VOI. The fractional volume of osmium-stained fat within the VOIs was determined using the Scanco 3D bone morphometry evaluation program with a threshold of 420 (1/1000 scale) and Gaussian filtering ( $\sigma=0.8$ , support=1). The data can be expressed as adipocyte volume/total volume (AV/TV) (Fig. 7.5). This volumetric adipocyte measurement is analogous to the volumetric bone measurement, BV/TV.

*Note:* These VOIs are based on the literature and our experience (Gimble, Zvonic, Floyd, Kassem, & Nuttall, 2006; Meunier, Aaron, Edouard, & Vignon, 1971; Moore & Dawson, 1990). As MAT increases in the medullary canal of the long bones it accumulates in a directed fashion. For the tibia, from the proximal end distally and for the femur, from the distal end proximal.

Because the bones are fixed in buffered formalin, they can be imaged by micro-CT to obtain cortical and trabecular bone measurements. Once accomplished, the bones can then be decalcified and osmium stained. This allows for a direct comparison, in the same bone, to measure bone and MAT parameters (i.e., medullary canal volume).

Our variability from experiment to experiment when comparing the same bones from the same strain is low. This is especially true when all of the processing (fixation, decalcification, osmium staining, and imaging) is done by the same group of investigators. We attribute the variability we do see to small changes in the processing and individual animal variability (even with the same bones from other mice of the same strain, in the same

experiment). Larger variability is seen when the mice are manipulated to change MAT (e.g., high-fat diet, calorie restriction, irradiation). It is unlikely that the variability is due to the imaging component of the method. This suggests that with experience, a single group of investigators will have less variability (practice makes perfect).

#### 4. SUMMARY

This chapter presents a new method for the visualization and quantification of MAT. This method is based on the specific staining of lipid by osmium tetroxide, which is detected and quantitated by micro-CT. This method relies on the decalcification of bone and has been successfully used on mouse long bones. The vast majority of the staining is in mature adipocytes not in other BM cells. In addition to quantitation of BM adipocytes, this method provides a 3D map of the MAT throughout the medullary canal and above the growth plate in the secondary center of ossification. This approach is rapid, reproducible, and quantitative.

#### Acknowledgments

We thank Dr. Douglas Adams, University of Connecticut Health Science Center, Farmington, CT for his valuable input and Michelle Lynch, University of Michigan, Ann Arbor, MI for helpful discussions. The Horowitz laboratory is partially supported by NIH Grants DK092759, AR046032, and the Department of Orthopaedics and Rehabilitation, Yale University School of Medicine. The MacDougald laboratory is partially supported by NIH Grants DK092759, DK062876, and DK95705.

#### References

- Bathija A, Davis S, Trubowitz S. Bone marrow adipose tissue: Response to acute starvation. *American Journal of Hematology*. 1979; 6:191–198. [PubMed: 484542]
- Berry R, Rodeheffer MS. Characterization of the adipocyte cellular lineage in vivo. *Nature Cell Biology*. 2013; 15:302–308.
- Bredella MA, Fazeli PK, Miller KK, Misra M, Torriani M, Thomas BJ, et al. Increased bone marrow fat in anorexia nervosa. *The Journal of Clinical Endocrinology and Metabolism*. 2009; 94:2129–2136. [PubMed: 19318450]
- Custer RP. Studies on the structure and function of bone marrow. Part I. *The Journal of Laboratory and Clinical Medicine*. 1932; 17:951–960.
- Custer RP, Ahlfeldt FE. Studies on the structure and function of bone marrow II. *The Journal of Laboratory and Clinical Medicine*. 1932; 17:960–962.
- Demontiero O, Li W, Thembani E, Duque G. Validation of noninvasive quantification of bone marrow fat volume with microCT in aging rats. *Experimental Gerontology*. 2011; 96:435–440. [PubMed: 21256205]
- Devlin MJ, Cloutier AM, Thomas NA, Panus DA, Lotinun S, Pinz I, et al. Caloric restriction leads to high marrow adiposity and low bone mass in growing mice. *Journal of Bone and Mineral Research*. 2010; 25:2078–2088. [PubMed: 20229598]
- Emery JL, Follett GF. Regression of bone-marrow haemopoiesis from the terminal digits in the foetus and infant. *British Journal of Haematology*. 1964; 10:485–489. [PubMed: 14218450]
- Evans JD, Riemenschneider RW, Herb SF. Fat composition and in vitro oxygen consumption of marrow from fed and fasted rabbits. *Archives of Biochemistry and Biophysics*. 1954; 53:157–166. [PubMed: 13208292]
- Fazeli PK, Horowitz MC, Macdougald OA, Scheller EL, Rodeheffer MS, Rosen CJ, et al. Marrow fat and bone—New perspectives. *The Journal of Clinical Endocrinology and Metabolism*. 2013; 98:935–945. [PubMed: 23393168]

- Fretz JA, Nelson T, Xi Y, Adams DJ, Rosen CJ, Horowitz MC. Altered metabolism and lipodystrophy in the Ebf1-deficient mouse. *Endocrinology*. 2010; 151:1611–1621. [PubMed: 20172967]
- Gimble JM, Zvonic S, Floyd ZE, Kassem M, Nuttall ME. Playing with bone and fat. *Journal of Cellular Biochemistry*. 2006; 98:251–266. [PubMed: 16479589]
- Huggins C, Blocksom BH Jr. Changes in outlying bone marrow accompanying a local increase of temperature within physiological limits. *The Journal of Experimental Medicine*. 1936; 64:253–274. [PubMed: 19870534]
- Kramer B, Shipley PG. Decalcification of bone in acid free Solutions. *Science*. 1927; 66:484–485. [PubMed: 17843739]
- Lillie RD. Studies on the decalcification of bone. *The American Journal of Pathology*. 1944; 20(2): 291–296. [PubMed: 19970755]
- Meunier P, Aaron J, Edouard C, Vignon G. Osteoporosis and the replacement of cell populations of the marrow by adipose tissue. A quantitative study of 84 iliac bone biopsies. *Clinical Orthopaedics*. 1971; 80:147–154.
- Moitra J, Mason MM, Olive M, Krylov D, Gavrilova O, Marcus-Samuels B, et al. Life without white fat: A transgenic mouse. *Genes & Development*. 1998; 12:3168–3181. [PubMed: 9784492]
- Moore SG, Dawson KL. Red and yellow marrow in the femur: Age-related changes in appearance at MR imaging. *Radiology*. 1990; 175:219–223. [PubMed: 2315484]
- Naveiras O, Nardi V, Wenzel PL, Hauschka PV, Fahey F, Daley GQ. Bone-marrow adipocytes as negative regulators of the haematopoietic microenvironment. *Nature*. 2009; 460:259–263. [PubMed: 19516257]
- Oehlbeck LWF, Robscheit-Robbins FS, Whipple GH. Marrow hyperplasia and hemoglobin reserve in experimental anemia due to bleeding. *The Journal of Experimental Medicine*. 1932; 56:425–428. [PubMed: 19870076]
- Palade GE. A study of fixation for electron microscopy. *The Journal of Experimental Medicine*. 1952; 95:285. [PubMed: 14927794]
- Ranvier, LA. *Traite technique d'histologie*. Paris: F. Savy; 1889. p. 264
- Regis-Arnaud A, Guui B, Walker PM, Krause D, Ricolfi F, Ben Salem D. Bone marrow fat quantification of osteoporotic vertebral compression fractures: Comparison of multi-voxel proton MR spectroscopy and chemical-shift gradient-echo MR imaging. *Acta Radiologica*. 2011; 52:1032–1036. [PubMed: 21948596]
- Rodeheffer MS, Birsoy K, Friedman JM. Identification of white adipocyte progenitor cells in vivo. *Cell*. 2008; 135:240–249. [PubMed: 18835024]
- Shillingford JP. The red bone marrow in heart failure. *Journal of Clinical Pathology*. 1950; 3:24–39. [PubMed: 15404597]
- Shore, LS. *Bone marrow as an adipose tissue*. Philadelphia: Hahnemann Medical College; 1969.
- Tavassoli M. Differential response of bone marrow and extramedullary adipose cells to starvation. *Experientia*. 1974; 30:424–425. [PubMed: 4858192]
- Tavassoli M. Ultrastructural development of bone marrow adipose cell. *Acta Anatomica (Basel)*. 1976a; 94:65–77.
- Tavassoli M. Marrow adipose cells. Histochemical identification of labile and stable components. *Archives of Pathology & Laboratory Medicine*. 1976b; 100:16–18. [PubMed: 56163]
- Trubowitz S, Bathija A. Cell size and palmitate-1-14c turnover of rabbit marrow fat. *Blood*. 1977; 49:599–605. [PubMed: 843618]
- Wronski TJ, Smith JM, Jee WS. Variations in mineral apposition rate of trabecular bone within the beagle skeleton. *Calcified Tissue International*. 1981; 33:583–586. [PubMed: 6799169]
- Yeung DK, Griffith JF, Antonio GE, Lee FK, Woo J, Leung PC. Osteoporosis is associated with increased marrow fat content and decreased marrow fat unsaturation: A proton MR spectroscopy study. *Journal of Magnetic Resonance Imaging*. 2005; 22:279–285. [PubMed: 16028245]

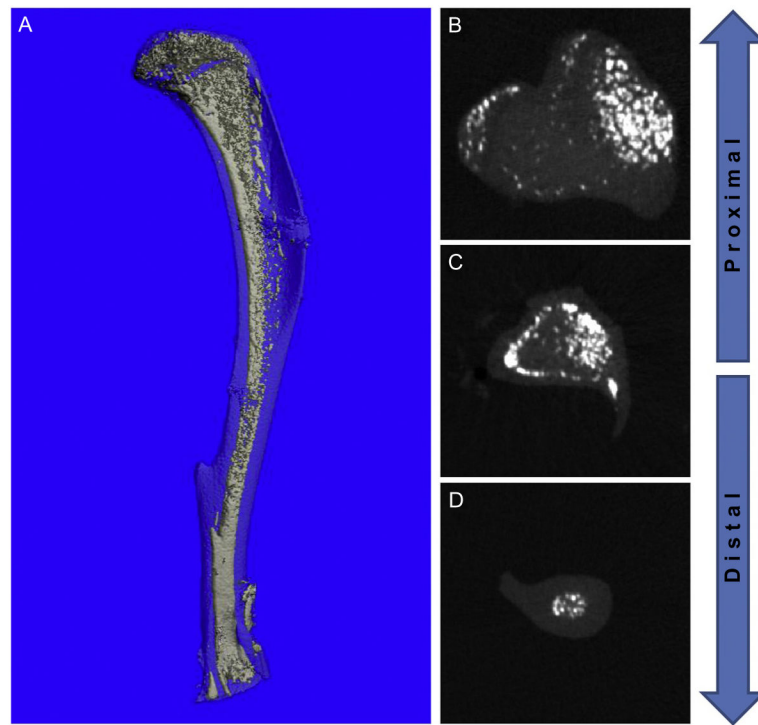


**Figure 7.1.**

Distribution of MAT in the medullary canal. Adipocytes in the BM of the mouse are unevenly distributed throughout the medullary canal. They are most densely clustered in the epiphyses. In the metaphysis and diaphysis, adipocytes are most numerous near the central vascular canal and adjacent to the cortical bone. (A) Three-dimensional reconstruction of a 16-week-old C3H mouse osmium-stained tibia. Light blue, bone; white, MAT. (B–D) Transverse sections of the same bone from more proximal (toward the knee) to distal (toward the ankle) showing defined regional clustering of the marrow adipocytes (white).

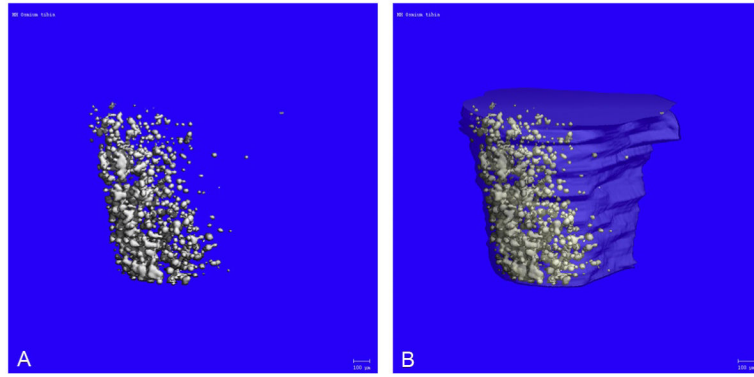


**Figure 7.2.**

Osmium-stained and micro-CT-imaged MAT from *Ebf1* null tibia. (A) Osmium-stained and micro-CT image of the proximal tibia from a 4-week-old *Ebf1*<sup>-/-</sup> mouse (no bone overlay). *Ebf1*<sup>-/-</sup> mice have very high MAT. (B) MAT from (A) with the bone overlaid.

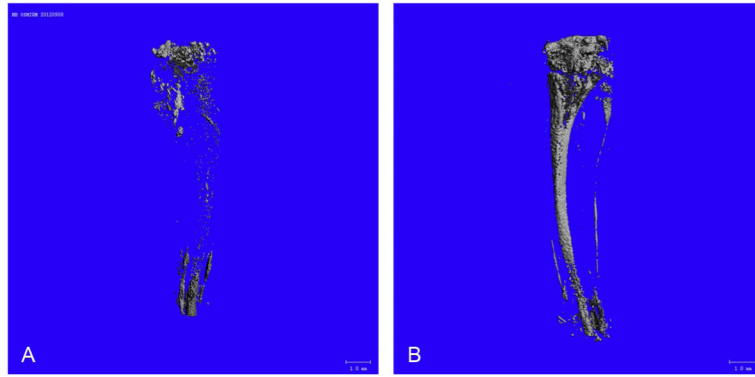


**Figure 7.3.**

Osmium-stained and micro-CT-imaged MAT from C57BL/6 and C3H/HeJ. (A) Osmium-stained and micro-CT image of the tibia from 15-week-old B6 mice (no bone overlay). (B) Osmium-stained and micro-CT image of the tibia from 15-week-old C3H mice (no bone overlay).

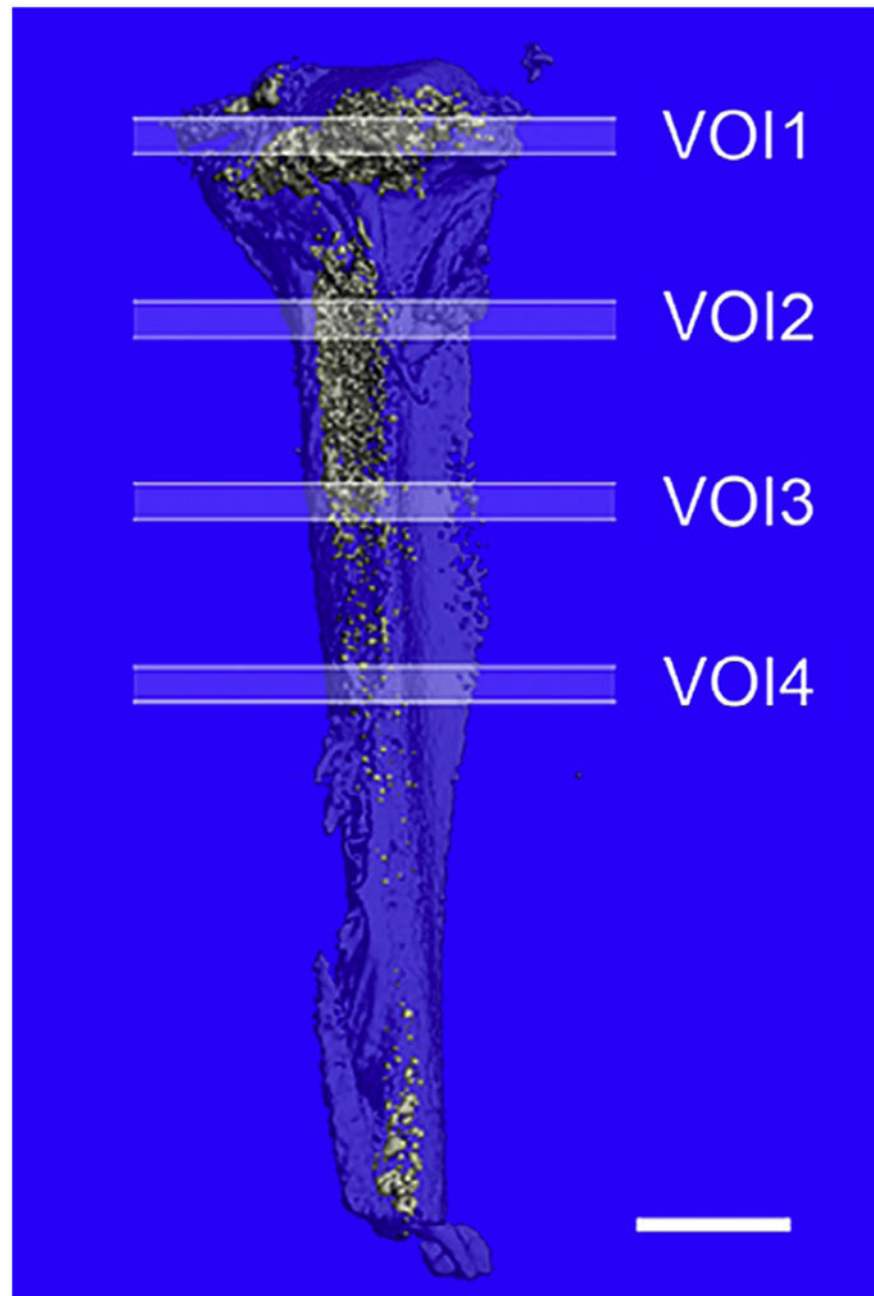


**Figure 7.4.**  
Positioning of the volumes of interest. VOIs in mouse femur.

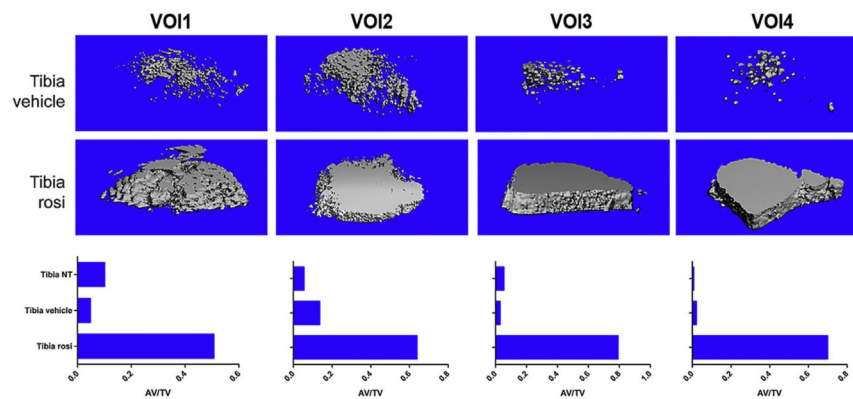


**Figure 7.5.**

Osmium-stained and micro-CT image of MAT from the femur of C57BL/6 mice fed a diet-containing rosiglitazone or control diet. B6 mice were fed a control diet or a diet-containing rosiglitazone for 8 weeks. Rosiglitazone is a PPAR $\gamma$  agonist and as such a potent inducer of MAT. The tibia was collected, stained with osmium tetroxide, and imaged with micro-CT. On control diet (vehicle) MAT is highest in VOI2 and decreases as you move distally down the shaft (VOIs 3 and 4). In contrast, mice on a rosiglitazone diet have very high MAT over the length of the tibial shaft.